AJNR

This information is current as of June 21, 2025.

Choroidal hemangioma: MR findings and differentiation from uveal melanoma.

C Stroszczynski, N Hosten, N Bornfeld, T Wiegel, A Schueler, P Foerster, A J Lemke, K T Hoffmann and R Felix

Choroidal Hemangioma: MR Findings and Differentiation from Uveal Melanoma

Christian Stroszczynski, Norbert Hosten, Norbert Bornfeld, Thomas Wiegel, Andreas Schueler, Paul Foerster, Arne Joern Lemke, Karl Titus Hoffmann, and Roland Felix

BACKGROUND AND PURPOSE: The aim of this study was to establish the MR imaging characteristics of choroidal hemangioma and to compare them with those of uveal melanoma.

METHODS: Among 41 patients examined at 1.5 T (4-cm surface coil, T1-weighted and fast spin-echo T2-weighted sequences), 25 had uveal melanoma and 16 had circumscribed choroidal hemangioma. After IV bolus injection of gadopentetate dimeglumine, dynamic and T1-weighted sequences were acquired.

RESULTS: In patients with choroidal hemangioma, uniform signal characteristics were detected on fast T2-weighted images. In 15 of 16 patients with choroidal hemangioma, lesions were isointense with vitreous on fast spin-echo T2-weighted images, whereas lesions in 24 of 25 patients with uveal melanoma were hypointense. Signal characteristics of uveal melanoma and hemangioma did not differ significantly on plain T1-weighted images. Enhancement was earlier and much stronger for circumscribed choroidal hemangioma than for uveal melanoma. After IV bolus application of gadopentetate dimeglumine, the increase of signal intensity was higher for circumscribed choroidal hemangioma (signal intensity ratio, 5.8) than for uveal melanoma (signal intensity ratio, 2.2).

CONCLUSION: Circumscribed choroidal hemangioma may be difficult to differentiate from melanoma by ophthalmologic examination. Differentiation may not be possible if direct viewing of uveal space-occupying lesions is hampered by opaque vitreous media. The characteristic findings on fast spin-echo T2-weighted MR images and early enhanced images aid in differentiating choroidal hemangioma from uveal melanoma.

The diagnosis of uveal tumors is usually possible by ophthalmoscopy, fluorescein angiography, or sonography. If direct viewing of the tumor is hampered by opaque vitreous media, a clinical diagnosis of a malignant lesion is not possible (1–5). Differential diagnosis of uveal space-occupying lesions can be supported by MR imaging (6–8).

Choroidal hemangioma is a benign vascular tumor of the choroid. Because the tumor is often concealed by retinal detachment, clinical diagnosis of choroidal hemangioma may be difficult. Furthermore, hemangioma may mimic other intraocular tumors. Uveal

melanoma is the most important differential diagnosis of circumscribed choroidal hemangioma in adults. To date, the MR appearance of uveal melanoma has been described in a number of reports, whereas few reports regarding the use of MR imaging in patients with choroidal hemangioma have been published (6, 8–10). The aim of this study was to evaluate the MR findings of choroidal hemangioma and to compare them with those of uveal melanoma.

Methods

Patients

A total of 41 patients, including two groups of patients with space-occupying lesions of the uvea, were examined prospectively by MR imaging. The first group included 16 patients with a clinical diagnosis of circumscribed choroidal hemangioma; the patients were treated in consecutive order during a period of 15 months at a referral center for ocular tumors. Acute loss of vision was detected in patients at clinical examination, or the lesions were discovered accidentally during ophthalmologic examination. The majority of patients (13 of 16) had typical ophthalmologic signs of choroidal hemangioma, such as an orangelike pattern, exudative retinal detachment, tumor vessels, and defects in the retinal epithelium overlying the tumor.

A diagnosis of choroidal hemangioma was doubtful after initial ophthalmologic examination in three of 16 cases but was eventually supported by the findings at sonography, fluorescein angiography, and follow-up examinations. A diagnosis of Sturge-Weber disease was not considered because the results of clinical and ophthalmologic examinations were supported by findings at CT or MR imaging of the brain.

The results were compared with those of 25 patients with an ophthalmologic diagnosis of uveal melanoma, who were included in consecutive order. Patients with general contraindications for MR imaging (ie, claustrophobia, pacemakers, metallic implants) were excluded from the study.

Examination Technique

All patients were examined at 1.5 T with a commercially available unit. A recently developed receive-only surface coil with a diameter of 4 cm, designed by the manufacturer, was used.

We used a standard T1-weighted spin-echo (SE) sequence with imaging parameters of 600/20/3 (TR/TE/excitations), a section thickness of 2 mm, a matrix of 256 × 256 pixels, and a field of view of 60 mm. A fast spin-echo (FSE) T2-weighted sequence (2000/70/1) with a section thickness of 2 mm, a matrix of 256 × 256 pixels, and a field of view of 120 mm was used. In all cases, enhanced studies with gadopentetate dimeglumine were performed.

After bolus injection of 0.1 mmol/kg of body weight of the contrast agent (11), dynamic studies were obtained with a T1-weighted SE sequence (150/20/1) using a section thickness of 2 mm, a matrix of 128 × 128 pixels, and a field of view of 60 mm. The acquisition time was 23 seconds per image; 13 consecutive images were obtained after bolus injection. Additional images were acquired 9 to 12 minutes after IV application. For postcontrast T1-weighted studies, all imaging parameters were kept identical to those used in the plain T1-weighted SE sequence.

Plain T1-weighted, FSE T2-weighted, and dynamic images were obtained in transverse orientation; postcontrast T1-weighted SE images were acquired in transverse plus sagittal or coronal planes. The signal intensity of lesions on plain T1-weighted SE images and FSE T2-weighted images was rated as very hypointense, hypointense, isointense, hyperintense, and very hyperintense relative to the vitreous, as proposed by Peyster et al (10).

Data analysis of contrast enhancement on dynamic images was performed with a region-of-interest technique. The regions of interest were placed in the uveal space-occupying lesion, including the maximum of pixels inside the lesion. Additionally, the mean intensities of background noise, including systematic and statistical noise, were measured outside the examined eye in a large region of interest. The signal-to-noise ratio (SNR) was calculated for each dynamic image and plotted against time. For each lesion, the increase in signal intensity over the baseline SNR was calculated as follows: signal intensity ratio = SNR_{max}/SNR_{plain}.

Results

MR Appearance of Circumscribed Choroidal Hemangioma on T1- and FSE T2-Weighted Images

In 16 patients with circumscribed choroidal hemangioma, all lesions were detected by MR imaging. The lesions were located in the posterior globe in all cases. In one case, choroidal hemangioma was not detected on T1-weighted sequences, and, in two other cases, no lesions were detected on FSE T2-weighted images. The signal characteristics of the lesions are summarized in Tables 1 and 2. On T1-weighted images, choroidal hemangiomas had a lentiform appearance with isointense or hyperintense structures as compared with the vitreous. On FSE T2-weighted images, choroidal hemangiomas were depicted as areas with homogeneous signal intensity similar to the vitreous in most cases (15 of 16). In one patient whose lesion was hypointense on FSE T2-weighted images, ophthalmologic findings were typical of choroidal hemangioma. Retinal detachment was infrequent

TABLE 1: MR signal intensity of the lesions in relation to vitreous*

Lesion Type	Very Hyperintense	Hyperintense	Isointense	Hypointense	Very Hypointense	Total
T1-weighted SE images						
Choroidal hemangioma	1	11	4			16
Uveal melanoma	4	21				25
FSE T2-weighted images						
Choroidal hemangioma			15	1		16
Uveal melanoma			1	11	13	25

Note.—SE indicates spin-echo; FSE, fast spin-echo.

* Lesions not visible on plain T1- or T2-weighted FSE images but clearly detectable after application of contrast agent were considered as isointense.

TABLE 2: Signal-to-noise ratios of choroidal hemangioma and uveal melanoma on dynamic T1-weighted spin-echo images

	SNR_plain		SNR_max		SI Ratio*		
	Mean	SD	Mean	SD	Median	Min	Max
Choroidal hemangioma	5.2	±2.3	32.4	±5.9	5.8	3.5	7.6
Uveal melanoma	2.2	±6.7	22.3	±7.8	2.2	1.3	3.8

Note.—SNR indicates signal-to-noise ratio; SI, signal intensity; min, minimal; max, maximal.

* SI ratio = SNR_{max}/SNR_{plain}.

TABLE 3: Characteristics of 16 patients with choroidal hemangioma

Patient	Age, y/Sex	Diameter (mm)	Protrusion (mm)	Visible Retina*	Retinal Detachment	Homogenity†	Comments
1	46/M	8.2	3.1	+	−	+	
2	13/F	10.1	4.8	−	+	+	
3	46/F	7.7	3.0	+	−	+	
4	29/M	5.9	2.2	+	−	+	
5	26/F	11.1	4.5	+	−	+	
6	39/F	5.0	1.5	+	−	−	Atypical MR appearance
7	44/M	4.3	2.3	−	−	+	
8	39/M	9.7	3.0	−	−	+	
9	49/M	7.6	2.5	−	−	+	
10	54/M	3.1	2.0	−	+	+	Associated large cyst
11	12/F	9.6	3.2	+	+	+	
12	09/F	10.1	4.8	+	+	+	
13	45/M	3.6	2.1	+	−	+	
14	19/F	8.4	4.3	−	+	+	Total ablation
15	52/M	6.7	3.0	+	−	+	
16	39/F	6.9	3.6	−	+	+	

Note.—FSE, indicates fast spin-echo; +, yes; −, no.

* Retina is visible on FSE T2-weighted images as bulging line into the vitreous.
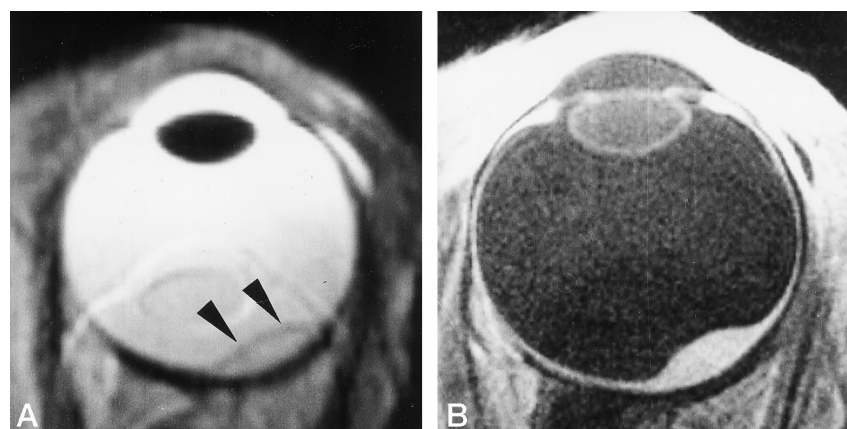
† Homogenity on T1-weighted contrast-enhanced images.

FIG 1. Appearance of choroidal hemangioma.

A, Axial FSE T2-weighted (2000/70/1) MR image shows that the overlying retina (*arrowheads*) becomes detectable despite ghosting.

B, Axial contrast-enhanced T1-weighted MR image (600/20/3) shows a high signal increase and homogeneous enhancement of the tumor.

(38%) (Table 3). If retinal detachment occurred, it was visible as a fine hypointense line on FSE T2-weighted images. The part of the retina overlying the hemangioma became visible on FSE T2-weighted images in 56% of the cases (Fig 1). Tumor size did not correspond to the appearance of retinal detachment or to the appearance of the adjoining retina on FSE T2-weighted images.

The maximal diameter of the tumors varied from 3.1 to 11.1 mm (average diameter, 7.5 mm). The majority had a lentiform appearance. The patient with the smallest hemangioma in this group (3.1 × 2.0 mm) had a cystic lesion close to the hemangioma.

In no patient was the sclera indented. MR imaging was considered helpful because of the typical characteristics of three patients in whom the diagnosis of choroidal hemangioma was doubtful after initial ophthalmologic examinations (Fig 2).

MR Appearance of Circumscribed Choroidal Hemangioma on Dynamic and Enhanced T1-Weighted Images

After IV bolus injection of the contrast agent, a strong and early enhancement was established in all choroidal hemangiomas, documented after the first or second dynamic image. The fill-in of hemangioma with contrast agent was characterized by a centrifugal direction in the distribution of contrast material in the lesions, documented in seven of 16 cases after the first or second dynamic image (Fig 3B and C). These images showed a sharp boundary in a tangential direction between the enhanced area close to the retina and the unenhanced area adjoining the sclera, followed by a homogenous appearance of the lesion on the next images. In nine of 16 cases, the documentation of the fill-in was missed by the dynamic acquisition, characterized by a homogeneous signal increase
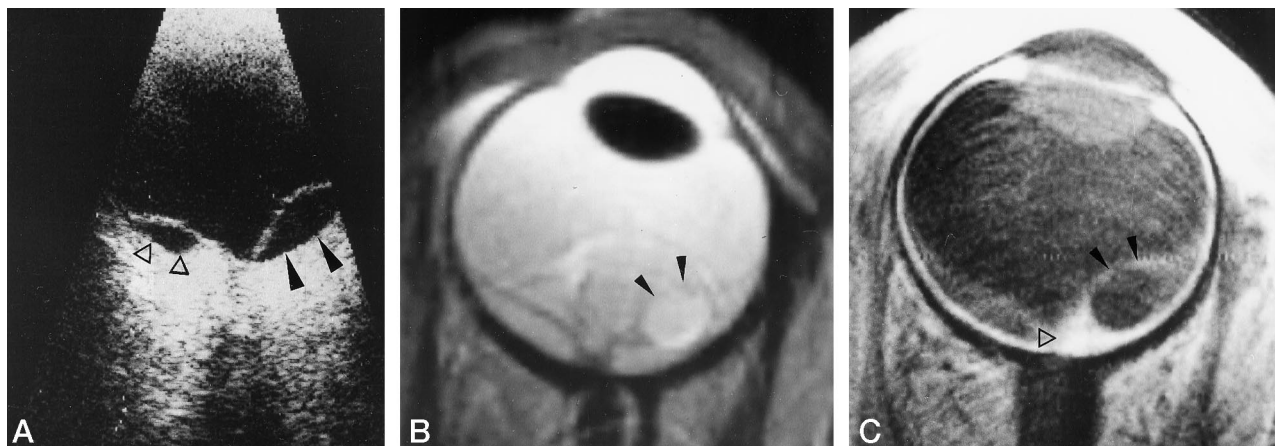
FIG 2.   46-year-old patient with acute loss of vision in the affected eye. After ophthalmoscopy and sonography, a choroidal cyst with retinal detachment was suspected.

A, Sonogram shows retinal detachment on the temporal side (*solid arrowheads*) and a cystic lesion on the nasal side (*open arrowheads*) of the posterior globe.

B, FSE T2-weighted (2000/70/1) MR image shows a large choroidal cyst (*arrowheads*) on the nasal side.

C, Contrast-enhanced T1-weighted image (600/20/3) shows a choroidal hemangioma (*open arrowhead*) containing a choroidal cyst (*solid arrowheads*). Both structures were isointense on FSE T2-weighted images, and a high increase of SNR was established after application of contrast agent. The diagnosis was circumscribed choroidal hemangioma.
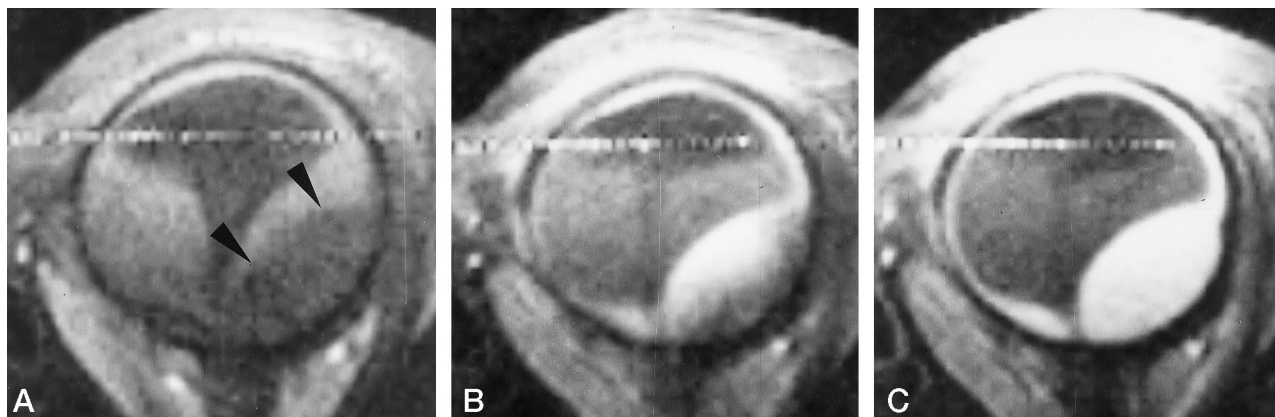

FIG 3.   Dynamic images (150/20/1) with a matrix of 128 $\times$ 128 pixels show the filling of a choroidal hemangioma after bolus application of contrast agent.

A, Plain T1-weighted SE image shows a choroidal hemangioma with retinal detachment and hyperintense subretinal effusion. Signal intensity of choroidal hemangioma (*arrowheads*) was low.

B, MR image 23 seconds after bolus injection shows the centrifugal direction of the distribution of contrast agent.

C, MR image at 46 seconds after injection shows the homogeneous filling of choroidal hemangioma.

of the whole lesion. The irregular enhancement pattern of choroidal hemangioma did not occur.

Maximal enhancement on dynamic MR images occurred during the 46- to 69-second time window, during which the average signal intensity ratio was 5.2, followed by a slow washout of contrast agent (Table 2). Ten minutes after the application of contrast agent, the SNR was still elevated threefold (Fig 4). In all patients, the relative increase in signal intensity of the hemangioma was higher than the increase in signal intensity of the uvea.

Comparison of Circumscribed Hemangioma and Uveal Melanoma

Although higher signal intensity was established on plain T1-weighted images for uveal melanoma than for choroidal hemangioma, signal intensity on plain T1-weighted images was not an accurate criterion for the differentiation because of an overlap of both entities in this respect (Table 1). In one of 25 patients with uveal melanoma, the tumor was isointense with respect to vitreous on FSE T2-weighted images. Using isointensity on FSE T2-weighted images as a criterion to differentiate choroidal melanoma from choroidal hemangioma, specificity was 93% and sensitivity was 96%. Irregular patterns were detected on early dynamic images of all uveal melanomas, whereas enhancement patterns 69 seconds after the application of contrast agent were uniform or irregular. The average signal intensity ratio was 2.2 and significantly lower ($P < .05$) than that for choroidal hemangioma (signal intensity ratio, 5.8) (Fig 4). If an increase of 3.5 in the signal intensity ratio was chosen
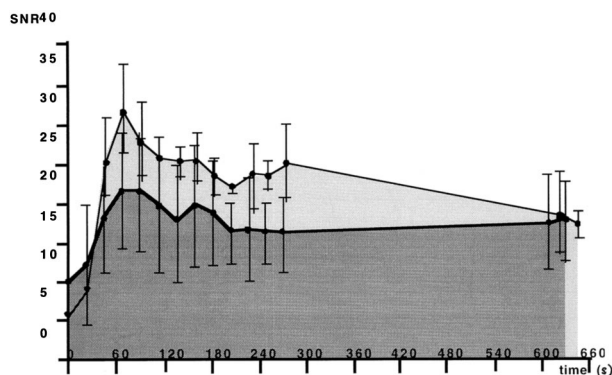
FIG 4. Mean values of SNRs of choroidal hemangioma (*thin line*) and uveal melanoma (*thick line*) measured by dynamic acquisition after bolus injection of contrast agent (T1-weighted SE images). Note that the mean SNR of uveal melanoma on plain T1-weighted images is significantly higher than that of choroidal hemangioma ($P < .05$). After bolus application of contrast agent, signal increase in choroidal hemangioma is higher than in uveal melanoma, while the washout is prolonged in both tumors.

as a cutoff level for differentiating choroidal hemangioma from uveal melanoma, then sensitivity for choroidal hemangioma was 100% and specificity was 88%.

Discussion

Choroidal hemangiomas may occur sporadically or in combination with Sturge-Weber disease (7). In cases of associated signs—that is, facial nevus flammeus, ipsilateral cutaneous lesions, or bilateral ocular signs and findings of venous hemangioma of the leptomeninges (encephalotrigeminal syndrome)—the diagnosis can be made easily. Circumscribed choroidal hemangioma is defined as a benign vascular tumor of the choroid that is not associated with Sturge-Weber syndrome (6).

Mainly located posterior to the equator, the tumor appears as a sometimes poorly defined, amelanotic, red-orange lesion (Fig 5). Tumor vessels lead to typical early filling at fluorescein or indocyanine-green angiography (4, 11). However, clinical differentiation of choroidal hemangioma from other amelanotic lesions is considered difficult (3, 5).

Uveal melanoma is the most frequent primary ocular malignant lesion in adult white patients and needs to be differentiated from choroidal hemangi-

oma. Although ophthalmologic examination is usually accurate in a diagnosis of uveal melanoma, clinical differentiation from choroidal hemangioma may be difficult, especially in cases of amelanotic melanoma. Furthermore, when opaque ocular media preclude a clear view or when vitreous hemorrhage and subretinal effusion obscure ophthalmoscopic viewing, differentiation from other uveal space-occupying lesions (choroidal metastasis, choroidal hemorrhage, age-related macular degeneration with retinal detachment, choroidal nevus, and melanocytoma) may not be possible (1, 2, 5, 12). Uveal leiomyoma or the rare intraocular hemangiopericytoma can be confused with amelanotic melanoma or hemangioma, whereas choroidal osteoma usually can be differentiated by sonography and CT because of typical calcification (6).

Differentiation of Circumscribed Choroidal Hemangioma and Uveal Melanoma by MR Imaging

The MR appearance of circumscribed choroidal hemangioma has been described in few reports (6, 8, 10). In agreement with our results in 16 patients, the majority of choroidal hemangiomas described in those articles were characterized by hyperintensity on T1-weighted SE images, whereas isointensity with the vitreous on FSE T2-weighted sequences was a constant finding. At 1.5 T, characteristic MR features of uveal melanoma showed, in the vast majority, hyperintensity on T1-weighted SE images and hypointensity on FSE T2-weighted images with respect to the vitreous. On the basis of a study of 43 patients, De Potter et al (6) reported that in fewer than 5% of patients with uveal melanoma, the tumor was hyperintense on T1-weighted SE images and isointense on T2-weighted SE images. Early MR studies have described the paramagnetic effects of melanin. The shortening of both T1- and T2-weighted relaxation time induces an increase in signal intensity on T1-weighted images and a decrease on T2-weighted images (10, 11).

We found that high signal intensity (isointense with vitreous) on FSE T2-weighted images was the most characteristic MR feature of choroidal hemangioma. However, especially in cases of amelanotic melanoma, signal intensity on FSE T2-weighted images
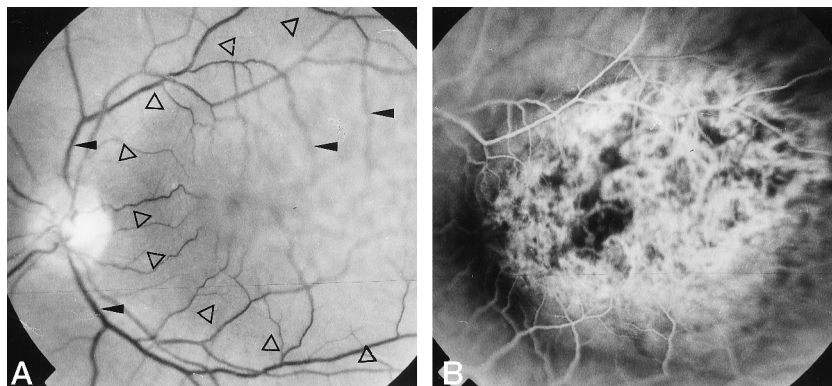

FIG 5. Typical ophthalmoscopic appearance of choroidal hemangioma.

A, Angiogram shows the well-defined round margins of the tumor (*open arrowheads*) and the less sharp demarcation of the overlying retinal vessels (*solid arrowheads*).

B, Fluorescein angiogram shows hypervascularization of the choroidal hemangioma.
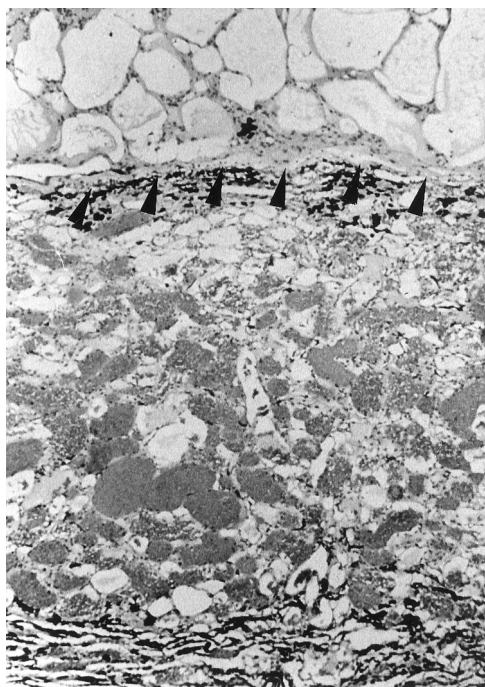
FIG 6. Microscopic view of a choroidal hemangioma (hematoxylin-eosin; original magnification, ×100). Note the cystic degeneration of the retina (*top*), which caused retinal enlargement. The margin between the retina and choroid is marked by *arrowheads*. The choroidal hemangioma with enlarged vessels is located in the middle of this view.

might be similar to choroidal hemangioma. In the majority of the patients with choroidal hemangioma, the overlying retinas became visible as a convex line on FSE T2-weighted sequences, whereas differentiation between the retinas and choroids of healthy patients is not possible even on high-resolution MR images. Fibrous metaplasia of the overlying retinal pigment epithelium (3, 6) and cystic degeneration causing thickening of the retina, as shown in Figure 6, may be the reasons the retina became detectable, whereas the variability of degeneration and enlargement may explain why, in other cases, overlying retinas were missed on FSE T2-weighted images.

When present, a well-defined centrifugal pattern of enhancement caused by the abundant tumor vessels of choroidal hemangioma was another sign that was useful for distinguishing between the two types of tumor. Because of the short fill-in period, the sign was presumably missed in nine of 16 patients on dynamic images. Further investigations will show whether gradient-echo sequences with shorter repetition times might solve the problem.

Uveal melanoma, in which abundant tumor vessels are detected by fluorescein or indocyanine angiography (4, 13), does not enhance as strongly as choroidal hemangioma, and signal intensity increases to a lesser extent after injection of contrast agent. Greater enhancement of choroidal hemangiomas as compared with melanomas on static MR images has been described previously in a limited number of patients (6, 8).

According to the data of dynamic studies, an optimal time window between 46 and 69 seconds occurs after bolus injection of contrast agent. Because of this limited available time, the acquisition of dynamic images seems to be an adequate means of quantifying signal increase for use as a valuable parameter in the differential diagnosis of space-occupying lesions. The acquisition of five dynamic images (at 0, 23, 46, 69, and 92 seconds after contrast injection) might be sufficient, because the dynamic images obtained after this time did not offer additional information.

The patterns of uveal melanomas, especially on early dynamic images, are irregular compared with the well-defined centrifugal or homogeneous patterns of choroidal hemangiomas. Hemorrhage, which that may change the signal characteristics of lesions, does not occur in choroidal hemangioma.

Although the destruction of Bruch's membrane associated with a mushroom-shaped infiltration into the vitreous is typical of uveal melanoma, it rarely occurs in patients with choroidal hemangioma (14). Whereas extraocular growth detected by MR imaging is observed in 10% to 15% of all cases of uveal melanoma (9), extraocular growth of choroidal hemangioma should not occur. Shape does not seem to be a useful sign for the differential diagnosis of choroidal hemangioma, since other tumors may be lentil-shaped as well.

Sonography is a valuable and cost-effective method for differentiating both tumors on the basis of the hyperreflectivity of choroidal hemangioma and the hypoechogenicity of the majority of uveal melanomas (12, 15). However, accuracy depends on the location of the uveal space-occupying lesions as well as on the experience of the operator, and results might be less accurate in cases of extensive ocular bleeding or necrosis (12, 15). Contrast-enhanced MR imaging is able to reflect the perfusion of intraocular space-occupying lesions and provides additional information for the differential diagnosis.

Conclusion

Isointensity on FSE T2-weighted images, combined with strong and early contrast enhancement, aids in the accurate differentiation of choroidal hemangioma from uveal melanoma.

References

1. Ferry AP. **Lesions mistaken for malignant melanoma of the posterior uvea: a clinico-pathologic analysis of 100 cases with ophthalmoscopically visible lesions.** *Arch Ophthalmol* 1964;72:463–467
2. Mauriello JA, Zimmerman LE, Rothstein TB. **Intrachoroidal hemorrhage mistaken for malignant melanoma.** *Ann Ophthalmol* 1983; 15:282–284
3. Nguyen AT, Anderson SF, Townsend JC. **Circumscribed choroidal hemangioma.** *J Am Optom Assoc* 1995;66:640–645
4. Piccolino FC, Borgia L, Zinicola E. **Indocyanine green angiography of circumscribed choroidal hemangiomas.** *Retina* 1996;16:19–28
5. Shields JA. **Lesions simulating malignant melanoma of the posterior uvea.** *Arch Ophthalmol* 1973;89:466–471
6. De Potter P, Shields JA, Shields CL. **Computed tomography and magnetic resonance imaging in intraocular lesions.** *Ophthalmol Clin North Am* 1994;7:333–346

7. Griffiths PD, Boodram MB, Blaser S, et al. **Abnormal ocular enhancement in Sturge-Weber syndrome: correlation of ocular MR and CT findings with clinical and intracranial imaging findings.** *AJNR Am J Neuroradiol* 1996;17:749–754

8. Mafee MF, Peyman GA, McKusick MA. **Malignant uveal melanoma and similar lesions: MR imaging evaluation.** *Radiology* 1986; 160:773–780

9. Hosten N, Lemke AJ, Sander B, et al. **MR anatomy and small lesions of the eye: improved delineation with a special surface coil.** *Eur Radiol* 1997;7:459–463

10. Peyster RG, Augsburger JJ, Shields JA, Hershey BL, Eagle R, Haskin ME. **Intraocular tumors: evaluation with MR imaging.** *Radiology* 1988;168:773–779

11. Gomori JM, Grossman RI, Shields JA, et al. **Choroidal melanomas:** correlation of NMR spectroscopy and MR imaging. *Radiology* 1986; 158:443–445

12. Verbeek AM, Koutentakis P, Deutman AF. **Circumscribed choroidal hemangioma diagnosed by ultrasonography: a retrospective analysis of 40 cases.** *Int Ophthalmol* 1996;19:185–189

13. Shields CL, Shields JA, De Potter P. **Patterns of indocyanine green videoangiography of choroidal tumours.** *Br J Ophthalmol* 1995;79: 237–245

14. Spraul CW, Kim D, Fineberg, E Grossniklaus HE. **Mushroom-shaped choroidal hemangioma.** *Am J Ophthalmol* 1996;122:434–436

15. Brab M, Adam G, Reim M, Günther RW. **Differential intraocular tumor diagnosis in MRI using gadolinium DTPA: value in comparison with other ophthalmologic examination procedures.** *Fortschr Ophthalmol* 1991;88:35–58